

Extremely Fast NADH-Regeneration Using Phosphonic Acid as Hydride Source and Iridium-Pyridin-2-Sulfonamidate Catalysts

Leonardo Tensi, and Alceo Macchioni

ACS Catal., Just Accepted Manuscript • DOI: 10.1021/acscatal.0c02261 • Publication Date (Web): 29 Jun 2020

Downloaded from pubs.acs.org on July 2, 2020

Just Accepted

“Just Accepted” manuscripts have been peer-reviewed and accepted for publication. They are posted online prior to technical editing, formatting for publication and author proofing. The American Chemical Society provides “Just Accepted” as a service to the research community to expedite the dissemination of scientific material as soon as possible after acceptance. “Just Accepted” manuscripts appear in full in PDF format accompanied by an HTML abstract. “Just Accepted” manuscripts have been fully peer reviewed, but should not be considered the official version of record. They are citable by the Digital Object Identifier (DOI®). “Just Accepted” is an optional service offered to authors. Therefore, the “Just Accepted” Web site may not include all articles that will be published in the journal. After a manuscript is technically edited and formatted, it will be removed from the “Just Accepted” Web site and published as an ASAP article. Note that technical editing may introduce minor changes to the manuscript text and/or graphics which could affect content, and all legal disclaimers and ethical guidelines that apply to the journal pertain. ACS cannot be held responsible for errors or consequences arising from the use of information contained in these “Just Accepted” manuscripts.

Extremely Fast NADH-Regeneration Using Phosphonic Acid as Hydride Source and Iridium-Pyridin-2-Sulfonamidate Catalysts

Leonardo Tensi^a and Alceo Macchioni^{*,a}

^a Dipartimento di Chimica, Biologia e Biotecnologie and CIRCC, Università degli Studi di Perugia, Via Elce di Sotto, 8-06123 Perugia, Italy

KEYWORDS NADH regeneration, iridium, homogeneous catalysis, transfer hydrogenation, bioinorganic chemistry.

ABSTRACT: NADH is a very well known, high-energy, electron and proton carrier, successfully employed as cofactor in many large-scale biotransformation processes catalyzed by oxidoreductase enzymes. Owing to its high cost, NADH has to be necessarily regenerated from cheap and affordable raw materials. Herein, we show that the combination of the [Cp*Ir(R-pysa)NO₃] (pysa = Π^2 -pyridine-2-sulfonamidate; R = H, 4-CF₃, and 6-NH₂) complexes and H–P(O)(OH)₂ as hydride source constitutes a top performing system for the chemical regeneration of NADH. Particularly, the enhanced metal acidity induced by the electron-withdrawing –S(O)₂– bridge, between the –NH amide functionality and the pyridine-ring, and the presence of the –NH₂ substituent in proximity to the metal are the key factors for obtaining the highest activity ever reported for the chemical regeneration of NADH (TOF up to 3731 h⁻¹, T = 313 K, pH = 6.58 by 0.4 M phosphite buffer), approaching that of enzymes.

NADH (Nicotinamide Adenine Dinucleotide in the reduced form) is an essential and ubiquitous coenzyme that plays a central role in several energy conversion processes of living organisms and in a large variety of redox reactions, where it acts as intracellular electron and hydrogen carrier. It is also used in many biocatalytic processes for the large-scale production of biofuels, chemicals and pharmaceuticals.^{1,2}

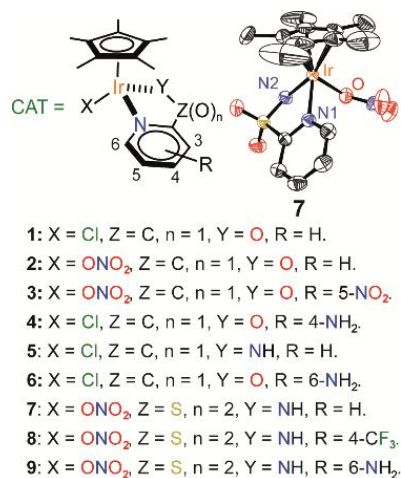
Due to its high cost,³ the utilization of NADH for industrial applications is necessarily related to the possibility of its catalytic regeneration from the oxidized form, NAD⁺,^{4,5,6} by the reaction with easily affordable reducing agents, such as formic acid [HC(O)OH]⁷ or phosphonic acid [HP(O)(OH)₂].^{8,9} Usually, the regeneration of NADH is mediated by enzymes, which exhibit remarkable efficiency and selectivity, but suffer from being not very stable and operating only under limited experimental conditions. Organometallic complexes, in combination with HC(O)OH, have been also proposed as robust and versatile catalysts for NADH regeneration^{10,11,12,13,14} but, unfortunately, their performances in term of efficiency and selectivity are much lower than those of enzymes so far.

Herein we report on a class of half-sandwich iridium(III) catalysts (CAT, Scheme 1) able to selectively regenerate the cofactor NADH with top activity (**7-9**, Scheme 1), approaching that of enzymes, when combined as H–P(O)(OH)₂ as hydride source, according to the following equation:



To the best of our knowledge, this is also the first example of hydrogenation of NAD⁺ using phosphonic acid as reducing agent mediated by an organometallic catalyst.

Complexes **1-9** were synthesized by the reaction of the iridium precursors [Cp*IrCl(μ-Cl)]₂ (**1-2**,¹⁵ **4**, **5**,¹⁶ **6**) or [Cp*Ir(H₂O)₃][NO₃]₂ (**3**, **7-9**) with 1 eq. of the appropriate ligand *per* Ir atom, in methanol at room temperature, in presence of 1 eq. of KOH (details are reported in the Supporting Information, SI). They were characterized in solution by multinuclear and multidimensional NMR techniques and by mass spectrometry (SI). Crystals of good quality for X-Ray diffractometric studies were obtained for complex **7** by slow diffusion of pentane into a saturated solution of **7** in dichloromethane (Scheme 1, SI).



Scheme 1. List of catalysts used in this work and ORTEP drawing of complex **7** (ellipsoid are drawn at 50% of probability, hydrogen atoms are omitted for clarity). Relevant distances (Å) and angles (°): Ir-Cp* = 1.776, Ir-O = 2.140 (2), Ir-N1 = 2.124 (2), Ir-N2 = 2.109 (2), N1-Ir-N2 = 81.28 (9), Cp*-Ir-N2 = 130.23 and Cp*-Ir-O = 128.30.

The catalytic activity of **1-9** in the regeneration of NADH was evaluated at 313 K and pH = 6.58 (by 0.4 M H₂PO₃⁻/HPO₃²⁻ buffer), following the appearance of the diagnostic UV-Vis band at 340 nm of NADH (Figure 1, SI).

The activity of carboxylate complexes (Z = C, Scheme 1) was critically affected by the nature and position of the R-substituent leading to following order:

3 (R = 5-NO₂) > **6** (R = 6-NH₂) > **2** (R = H) >> **4** (R = 4-NH₂)

It can be explained assuming that: 1) an electron-withdrawing substituent, as 5-NO₂, has a beneficial effect in the catalytic activity, since it enhances the acidity of the complexes (the turnover frequency, TOF, evaluated as indicated in SI, passed from 94 h⁻¹ for **2** up to 291 h⁻¹ for **3**, Figure 1), as previously observed by Yoon and co-workers investigating Cp*Rh catalysts bearing CH₂OH-disubstituted bipyridine;¹⁷ 2) the presence of a base in proximity to iridium, as NH₂ in **6** (but not in **4**), facilitates the catalytic process; 3) the nature of the X-anion plays a marginal role, as indicated by the similar catalytic activity of **1** (TOF = 70 h⁻¹, X = Cl) and **2** (TOF = 94 h⁻¹, X = NO₃). Perhaps, point 2) is the least expected and, probably, the most intriguing because it allows rationalizing the observation that **4** (TOF = 7 h⁻¹) and **6** (TOF = 102 h⁻¹), reasonably having the same electron density at the metal, markedly differ in their catalytic activity because the -NH₂ functionality is near iridium in **6**. A confirmation of the positive role exerted by a basic functionality close to Ir comes from a comparison of the catalytic activity of complex **5** (TOF = 133 h⁻¹), which is significantly higher than that of the carboxylate analogue **1** (TOF = 70 h⁻¹).

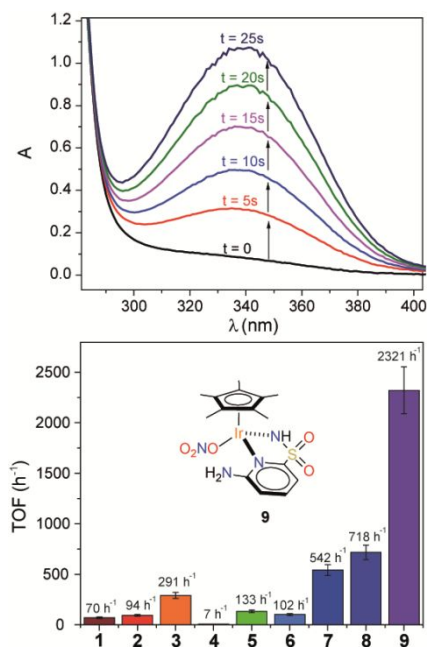


Figure 1. Below: TOF values for the studied catalysts under the following experimental conditions: [Cat] = 10 μM, [NAD⁺] = 0.77 mM, [H₂PO₃⁻/HPO₃²⁻] = 0.4 M, pH = 6.58, 313K. Above: Initial kinetics of the growth of the UV-Vis band at 340 nm typical of NADH.

Guided by those findings we searched for ligands that could impart higher acidity at the metal center, possibly decorated with a base near iridium. Our choice fell on pyridine-2-sulfonamide ligands.^{18,19,20} Particularly, three half-sandwich iridium(III) complexes, bearing R-pyridine-2-sulfonamide ligands (R-pysa) with different substituents (**7**, R = H; **8**, R = 4-CF₃; **9**, R = 6-NH₂; Scheme 1), were synthesized and tested as potential catalysts for NADH regeneration with HP(O)(OH)₂ (SI).

A ca. 4 times enhancement of activity was obtained by the introduction of the more electron withdrawing bridge between the pyridine and amide functionalities, i. e. passing from -C(O)- (**5**, TOF = 133 h⁻¹) to -S(O)₂- (**7**, TOF = 542 h⁻¹). A further depletion of electron density in the pyridine ring, due to the presence of a slightly electron withdrawing substituent, such as CF₃ in *para* position, was also beneficial (**8**, TOF = 718 h⁻¹). Nevertheless, the cooperative effect of the enhanced acidity at the metal center, induced by the pysa-ligands, and the presence of a dangling base functionality close to the metal appears to be the key for having top performing catalysts. This can be clearly appreciated by the jump of activity passing from **6** (TOF = 102 h⁻¹) to **9** (TOF = 2321 h⁻¹), ca. 22 times, which is much higher than that observed passing from **1** (TOF = 70 h⁻¹) to **6** (TOF = 542 h⁻¹), which is "only" ca. 8 times (Figure 1). In addition to this remarkable catalytic activity, [Cp*Ir(R-pysa)NO₃] complexes were also found to be chemoselective. This was demonstrated by monitoring the catalytic reaction by ¹H NMR spectroscopy ([NAD⁺] = 10.1

mM, **9**] = 100 μ M, buffer phosphite 0.4 M, pH = 6.58, T = 313 K). The disappearance of NAD⁺ resonances and the concomitant and exclusive appearance of the resonances of 1,4- β -NADH were observed (SI, Figure S21). The reaction went to completion [yield = 100 %, TON (moles of NADH/moles of **9**) = 101].

For the fastest catalyst **9**, a comparative experiment, aimed at investigating the effect of changing the hydrogen donor on the activity, was performed. Particularly, two kinetics of NAD⁺ hydrogenation, using alternatively H-COOH or H-P(O)(OH)₂ (0.1 M) as source of hydrogen, under the same experimental conditions ([**9**] = 5 μ M, [NAD⁺] = 0.77 mM, and pH 7, by 0.2 M phosphate buffer, T = 40 °C), were carried out. Interestingly, a four times higher TOF was obtained by using H-P(O)(OH)₂ (TOF = 1030 h⁻¹) instead of H-COOH (TOF = 266 h⁻¹), indicating that phosphonic acid is a superior source of hydrogen, at least for the investigated class of compounds.

In order to shed some light on the reaction mechanism of NADH regeneration with **7-9** catalysts, using H-P(O)(OH)₂ as hydride source, UV-Vis kinetic experiments were performed at various NAD⁺ concentrations (0.25 mM - 10 mM). It was found that after an initial beneficial effect of increasing NAD⁺ concentration on the reaction rate (r_{NADH}), suggesting NAD⁺ hydrogenation as the turnover limiting step, a further increase of NAD⁺ concentration caused a decrease of r_{NADH} , likely due to the NAD⁺ inhibitory effect related to its interaction with the catalyst (Figure 2, *vide infra* for further mechanistic considerations).¹⁶ It is important to notice that the maximum r_{NADH} occurs at higher NAD⁺ concentration for **9**, with respect to **7** and **8**. Furthermore, a less accentuated decrease of r_{NADH} with [NAD⁺] is observed for **9**, after the maximum (Figure 2).

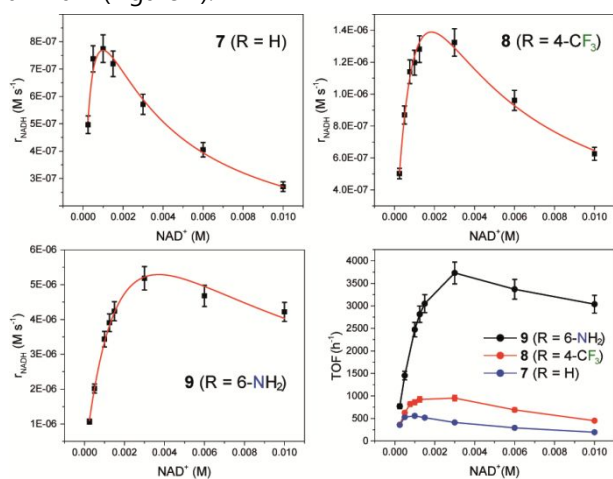
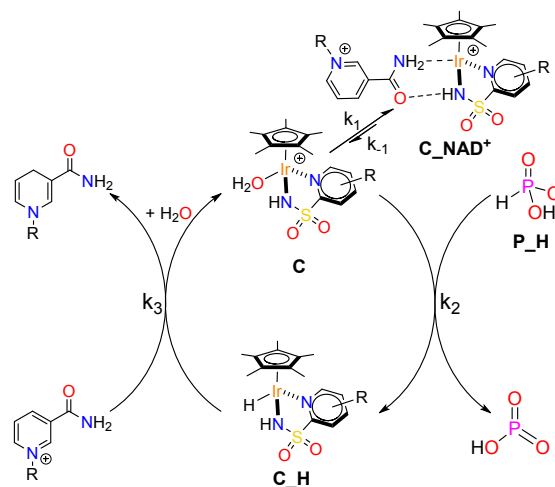


Figure 2. Plots r_{NADH} (M s⁻¹) vs. [NAD⁺] of catalysts **7** (up-left), **8** (up-right), **9** (down-left) and TOF vs. [NAD⁺] for catalysts **7-9** (down-right), under the following

experimental conditions: [CAT] = 5 μ M, [H₂PO₃⁻/HPO₃²⁻] = 0.4 M, pH = 6.58, 313K.

From previous studies is known^{21,22,23,16} that two chemical steps are the heart of NADH regeneration: 1) the formation of the metal hydride species (**C_H**) from the interaction of the pre-catalysts (**C**) with the hydride donor, H—P(O)(OH)₂ (**P_H**) in our case, and 2) the hydride transfer to NAD⁺ (Scheme 2). **C_H** was intercepted for **8** and **9** by dissolving the catalysts in a H₂PO₃⁻/HPO₃²⁻ buffered water solution in the absence of NAD⁺, which caused the instantaneous precipitation of **C_H** as a orange (**8_H**) and pale yellow (**9_H**) solid. The latter was dissolved in DMSO-d₆ and completely characterized by NMR (SI). It is also well known that the interaction between **C** and NAD⁺ might lead to a reversible and inhibiting out-of-cycle process, generating the **C_NAD**⁺ adduct (Scheme 2).¹⁶



Scheme 2. Proposed mechanism of hydrogenation of NAD⁺ with phosphonic acid with catalysts **7-9**.

Under the assumption that the reaction mechanism illustrated in Scheme 2 is operative, the mathematical equation relating r_{NADH} ($d[\text{NADH}]/dt$) to [NAD⁺] was obtained (Equation 1), imposing the steady state concentration to **C_H** and **C_NAD**⁺ (as detailed in SI).

$$r_{\text{NADH}} = \frac{k_2 k_3 [P_H] C_{\text{CAT}} [NAD^+]}{k_3 [NAD^+] + k_2 [P_H] + K_M k_3 [NAD^+]^2} \quad (1)$$

Fitting the trends r_{NADH} versus [NAD⁺] with Eq. 1 (Figure 2), k_2 , k_3 and the binding constant K_M (k_1/k_{-1}) were derived (Table 1). The results are reported in Table 1. They confirm that at low [NAD⁺] values the hydrogenation of NAD⁺ is always the turnover-limiting step since its velocity ($r_3 \propto k_3 [NAD^+]$) is lower than that **C_H** formation ($r_2 \propto k_2 [P_H]$), due to fact that $[P_H]/[NAD^+] > 100$. At higher [NAD⁺] values, instead, the formation of **C_H** becomes the turnover-limiting step ($r_3 > r_2$). At the same time, the coordination of NAD⁺ at the metal center, causes a decrease of r_{NADH} . As far as a comparative analysis of the **7-9** performances is concerned, the data in Table 1

suggest that catalyst **9** superiority is mainly due to its higher ability to form **C₂H** (k_2 is nine and three times larger than for **7** and **8**, respectively, Table 1) and to the lower tendency to generate the **C₂NAD⁺** out-of-cycle species (K_M is two times smaller than for **7** and **8**, Table 1, and more than one order of magnitude smaller than that previously determined for **5**¹⁶). As for the hydride transfer to NAD⁺ (k_3 in Table 1), **9** is still more active than other catalysts but the difference is less accentuated (k_3 is 1.4 and two times higher than for **7** and **8**, respectively, Table 1).

Table 1. Kinetic constants obtained by the fitting of the experimental data of catalysts 7-9 with Equation (1).

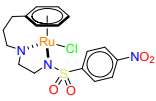
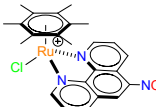
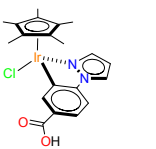
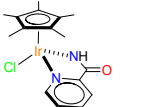

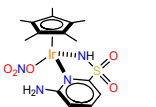
	7 (R = H)	8 (R = 4-CF ₃)	9 (R = 6-NH ₂)
k_3 (M ⁻¹ s ⁻¹)	687 ± 68	473 ± 23	970 ± 40
k_2 (M ⁻¹ s ⁻¹)	0.70 ± 0.06	1.90 ± 0.24	6.40 ± 0.83
K_M (M ⁻¹)	414 ± 57	474 ± 81	191 ± 44

It can be speculated that the presence of the -NH₂ functionality in six position of pyridine might properly orient H-P(O)(OH)₂ in a way of facilitating hydride transfer to iridium (high k_2), analogously to what occurs with Arg237 and His292 in PTDH (phosphite dehydrogenase) mediated NADH regeneration.²⁴ At the same time, the -NH₂ functionality might compete with the amide functionality of NAD⁺ for the occupancy of a coordination position at iridium, thus avoiding **C₂NAD⁺** formation (low K_M).

A remarkable TOF = 3731 h⁻¹ was measured in the experiment with [NAD⁺] = 3 mM for catalyst **9** (Figure 2, down-right, and SI). This value is the highest ever-reported TOF value for the catalytic regeneration of NADH carried out with a molecular organometallic catalyst as shown in Table 2. Despite the comparisons have to be taken with caution because of the different nature of the hydride source and different experimental conditions, Table 2 indicates that **9** (Table 2, entry 6) is by far much faster than all previously reported catalysts.²⁵ Only [Cp*Rh(phen)Cl]⁺ has a comparable TOF (2000 h⁻¹, Table 2, entry 5), even if it was measured at 60 °C, whereas that of **9** (3731 h⁻¹) at 40 °C. As shown in Table 2 (entries 7 and 8), enzymes still remain the fastest catalysts for NADH regeneration, nevertheless organometallic catalysts herein reported, having all the positive aspects of simple molecular catalysts in terms of stability and versatility of utilization, are approaching their performances.

Table 2. TOF values of some representative fast catalysts for the regeneration of NADH.

Entry	TOF (h ⁻¹)	Exp. Conditions
-------	------------------------	-----------------

1		9,9 ²⁶	[CAT] = 28 μM [NAD ⁺] = 0.17 mM [HCOONa] = 34 mM T = 37 °C, pH = 7.2
2		10 ²¹	[CAT] = 80 μM [NAD ⁺] = 8 mM [HCOONa] = 350 mM T = 38 °C, pH = 7
3		54 ²⁶	[CAT] = 15 μM [NAD ⁺] = 0.77 mM [HCOOK] = 120 mM T = 25 °C, pH = 7
4		143 ¹⁶	[CAT] = 7.5 μM [NAD ⁺] = 0.77 mM [HCOOK] = 125 mM T = 25 °C, pH = 7
5		2000 ²¹	[CAT] = 8 μM [NAD ⁺] = 8 mM [HCOONa] = 350 mM T = 60 °C, pH = 7
6		3731 This Work	[CAT] = 5 μM [NAD ⁺] = 3 mM [H ₂ PO ₃ ⁻ /HPO ₃ ²⁻] = 0.4 M T = 40 °C, pH = 6.58
7	FDH ^a	9000 ²⁷	[NAD ⁺] = 1.62 mM [HCOONa] = 162 mM T = 30 °C, pH = 7.5
8	PHD ^b	26280 ⁹	[NAD ⁺] = 1.00 mM [H ₃ PO ₃] = 1.00 mM T = 30 °C, pH = 7.25

^aFDH = phosphate dehydrogenase. ^bPTDH = phosphite dehydrogenase.

In conclusion, the system constituted by [Cp*Ir(R-pysa)NO₃] (especially when R = 6-NH₂) catalysts and H-P(O)(OH)₂ as hydride source appears to be extremely promising for the regeneration of NADH from its oxidized form NAD⁺; it approaches the catalytic activity of the most efficient enzymatic systems,^{8,9} with additional advantages in terms of simplicity of preparation and stability. The compatibility of utilization of **7-9** regeneration catalysts together with oxidoreductase enzymes,²⁸ in order to implement biocatalytic processes of industrial relevance, is under investigation in our laboratory. The results will be reported in the due course.

AUTHOR INFORMATION

Corresponding Author

*E-mail for A.M.: alceo.macchioni@unipg.it.

ORCID

A.M.: 0000-0001-7866-8332.

L.T.: 0000-0002-0966-6859.

Author Contributions

The manuscript was written through contributions of all authors.

ASSOCIATED CONTENT

Supporting Information. Details on materials and methods, synthesis and characterization of **3,6,7,8** and **9**, catalytic measurements, and kinetic equation are reported in a pdf file. A CIF file related to the X-Ray structure of **7** is also provided. "This material is available free of charge via the Internet at <http://pubs.acs.org>."

ACKNOWLEDGMENT

This work has been financially supported by PRIN 2015 (20154X9ATP_004), University of Perugia and MIUR (AMIS, "Dipartimenti di Eccellenza - 2018-2022" programs). We thank Chiara Taticchi, Vittorio Nofrini and Sybren Van Dijk for the preliminary syntheses of some complexes, and Dr. Simone Moretti and Prof. Gabriele Cruciani for the determination of the exact molecular mass of complexes **7-9**.

REFERENCES

(1) Atsumi, S.; Hanai, T.; Liao, J. C. Non-Fermentative Pathways for Synthesis of Branched-Chain Higher Alcohols as Biofuels. *Nature* **2008**, *451* (7174), 86–89. <https://doi.org/10.1038/nature06450>.

(2) Ma, S. K.; Gruber, J.; Davis, C.; Newman, L.; Gray, D.; Wang, A.; Grate, J.; Huisman, G. W.; Sheldon, R. A. A Green-by-Design Biocatalytic Process for Atorvastatin Intermediate. *Green Chem.* **2010**, *12* (1), 81–86. <https://doi.org/10.1039/b919115c>.

(3) Monti, D.; Ottolina, G.; Carrea, G.; Riva, S. Redox Reactions Catalyzed by Isolated Enzymes. *Chem. Rev.* **2011**, *111* (7), 4111–4140. <https://doi.org/10.1021/cr100334x>.

(4) Wu, H.; Tian, C.; Song, X.; Liu, C.; Yang, D.; Jiang, Z. Methods for the Regeneration of Nicotinamide Coenzymes. *Green Chem.* **2013**, *15* (7), 1773–1789. <https://doi.org/10.1039/c3gc37129h>.

(5) Wang, X.; Saba, T.; Yiu, H. H. P.; Howe, R. F.; Anderson, J. A. Cofactor NAD (P) H Regeneration Inspired by Heterogeneous Pathways. *Chem* **2017**, *2* (5), 621–654. <https://doi.org/10.1016/j.chempr.2017.04.009>.

(6) Wu, Y.; Shi, J.; Li, D.; Zhang, S.; Gu, B.; Qiu, Q.; Sun, Y.; Zhang, Y.; Cai, Z.; Jiang, Z. Synergy of Electron Transfer and Electron Utilization via Metal–Organic Frameworks as an Electron Buffer Tank for Nicotinamide Regeneration. *ACS Catal.* **2020**, *2894–2905*. <https://doi.org/10.1021/acscatal.9b05240>.

(7) Schutte, H.; Flossdorf, J.; Sahm, H.; Kula, M.-R. Purification and Properties of Formaldehyde Dehydrogenase and Formate Dehydrogenase from *Candida Boidinii*. *Eur. J. Biochem.* **1976**, *62* (1), 151–160. <https://doi.org/10.1111/j.1432-1033.1976.tb10108.x>.

(8) Vrtis, J. M.; White, A. K.; Metcalf, W. W.; Van der Donk, W. A. Phosphite Dehydrogenase: An Unusual Phosphoryl

Transfer Reaction. *J. Am. Chem. Soc.* **2001**, *123* (11), 2672–2673. <https://doi.org/10.1021/ja004301k>.

(9) Garcia Costas, A. M.; White, A. K.; Metcalf, W. W. Purification and Characterization of a Novel Phosphorus-Oxidizing Enzyme from *Pseudomonas Stutzeri* WM88. *J. Biol. Chem.* **2001**, *276* (20), 17429–17436. <https://doi.org/10.1074/jbc.M011764200>.

(10) Abril, O.; Whitesides, G. M. Hybrid Organometallic/Enzymatic Catalyst Systems: Regeneration of NADH Using Dihydrogen. *J. Am. Chem. Soc.* **1982**, *104* (6), 1552–1554. <https://doi.org/10.1021/ja00370a017>.

(11) Quinto, T.; Köhler, V.; Ward, T. R. Recent Trends in Biomimetic NADH Regeneration. *Top. Catal.* **2014**, *57* (5), 321–331. <https://doi.org/10.1007/s11244-013-0187-y>.

(12) Fukuzumi, S.; Lee, Y.-M.; Nam, W. Catalytic Recycling of NAD(P)H. *J. Inorg. Biochem.* **2019**, *199* (May), 110777. <https://doi.org/10.1016/j.jinorgbio.2019.110777>.

(13) Betanzos-Lara, S.; Liu, Z.; Habtemariam, A.; Pizarro, A. M.; Qamar, B.; Sadler, P. J. Organometallic Ruthenium and Iridium Transfer-Hydrogenation Catalysts Using Coenzyme NADH as a Cofactor. *Angew. Chemie Int. Ed.* **2012**, *51* (16), 3897–3900. <https://doi.org/10.1002/anie.201108175>.

(14) Okamoto, Y.; Ward, T. R. Transfer Hydrogenation Catalyzed by Organometallic Complexes Using NADH as a Reductant in a Biochemical Context. *Biochemistry* **2017**, *56* (40), 5223–5224. <https://doi.org/10.1021/acs.biochem.7b00809>.

(15) Bucci, A.; Savini, A.; Rocchigiani, L.; Zuccaccia, C.; Rizzato, S.; Albinati, A.; Llobet, A.; Macchioni, A. Organometallic Iridium Catalysts Based on Pyridinecarboxylate Ligands for the Oxidative Splitting of Water. *Organometallics* **2012**, *31*, 8071–8074. <https://doi.org/10.1021/om301024s>.

(16) Bucci, A.; Dunn, S.; Bellachioma, G.; Menendez Rodriguez, G.; Zuccaccia, C.; Nervi, C.; Macchioni, A. A Single Organoiridium Complex Generating Highly Active Catalysts for Both Water Oxidation and NAD + /NADH Transformations. *ACS Catal.* **2017**, *7* (11), 7788–7796. <https://doi.org/10.1021/acscatal.7b02387>.

(17) Ganesan, V.; Sivanesan, D.; Yoon, S. Correlation between the Structure and Catalytic Activity of [Cp*Rh(Substituted Bipyridine)] Complexes for NADH Regeneration. *Inorg. Chem.* **2017**, *56* (3), 1366–1374. <https://doi.org/10.1021/acs.inorgchem.6b02474>.

(18) Li, M.; Takada, K.; Goldsmith, J. I.; Bernhard, S. Iridium(III) Bis-Pyridine-2-Sulfonamide Complexes as Efficient and Durable Catalysts for Homogeneous Water Oxidation. *Inorg. Chem.* **2016**, *55* (2), 518–526. <https://doi.org/10.1021/acs.inorgchem.5b01709>.

(19) Li, M.; Bernhard, S. Synthetically Tunable Iridium(III) Bis-Pyridine-2-Sulfonamide Complexes as Efficient and Durable Water Oxidation Catalysts. *Catal. Today* **2017**, *290*, 19–27. <https://doi.org/10.1016/j.cattod.2016.11.027>.

(20) Tanaka, K.; Miki, T.; Murata, K.; Yamaguchi, A.; Kayaki, Y.; Kuwata, S.; Ikariya, T.; Watanabe, M. Reductive Amination of Ketonic Compounds Catalyzed by Cp*Ir(III) Complexes Bearing a Picolinamidato Ligand. *J. Org. Chem.* **2019**, *84* (17), 10962–10977. <https://doi.org/10.1021/acs.joc.9b01565>.

(21) Canivet, J.; Süß-Fink, G.; Štěpnička, P. Water-Soluble Phenanthroline Complexes of Rhodium, Iridium and Ruthenium for the Regeneration of NADH in the Enzymatic Reduction of Ketones. *Eur. J. Inorg. Chem.* **2007**, No. 30, 4736–4742. <https://doi.org/10.1002/ejic.200700505>.

1 (22) Soldevila-Barreda, J. J.; Bruijninx, P. C. A.;
2 Habtemariam, A.; Clarkson, G. J.; Deeth, R. J.; Sadler, P. J.
3 Improved Catalytic Activity of Ruthenium-Arene Complexes in
4 the Reduction of NAD⁺. *Organometallics* **2012**, *31* (16), 5958–
5967. <https://doi.org/10.1021/om3006307>.

5 (23) Maenaka, Y.; Suenobu, T.; Fukuzumi, S. Efficient
6 Catalytic Interconversion between NADH and NAD⁺
7 Accompanied by Generation and Consumption of Hydrogen
8 with a Water-Soluble Iridium Complex at Ambient Pressure and
9 Temperature. *J. Am. Chem. Soc.* **2012**, *134* (1), 367–374.
10 <https://doi.org/10.1021/ja207785f>.

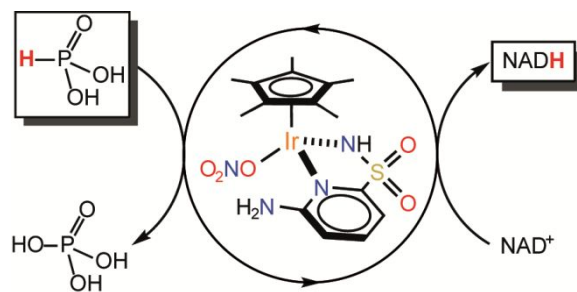
11 (24) Howe, G. W.; van der Donk, W. A. 18 O Kinetic Isotope
12 Effects Reveal an Associative Transition State for Phosphite
13 Dehydrogenase Catalyzed Phosphoryl Transfer. *J. Am. Chem.*
14 *Soc.* **2018**, *140* (51), 17820–17824.
15 <https://doi.org/10.1021/jacs.8b06301>.

16 (25) A remarkable activity was also observed covalently
17 immobilizing [Cp*Rh(bpy)Cl]⁺ onto the surface of a bucky paper
18 electrode: Zhang, L.; Etienne, M.; Vilà, N.; Le, T. X. H.; Kohring, G.
19 W.; Walcarius, A. Electrocatalytic Biosynthesis Using a Bucky
20 Paper Functionalized by [Cp*Rh(Bpy)Cl]⁺ and a Renewable
21 Enzymatic Layer. *ChemCatChem* **2018**, *10* (18), 4067–4073.
22 <https://doi.org/10.1002/cctc.201800681>.

23 (26) Chen, F.; Romero-Canelón, I.; Soldevila-Barreda, J. J.;
24 Song, J. I.; Coverdale, J. P. C.; Clarkson, G. J.; Kasparkova, J.;
25 Habtemariam, A.; Wills, M.; Brabec, V.; Sadler, P. J. Transfer
26 Hydrogenation and Antiproliferative Activity of Tethered Half-
27 Sandwich Organoruthenium Catalysts. *Organometallics* **2018**,
28 *37* (10), 1555–1566.
29 <https://doi.org/10.1021/acs.organomet.8b00132>.

30 (27) Slusarczyk, H.; Felber, S.; Kula, M. R.; Pohl, M.
31 Stabilization of NAD-Dependent Formate Dehydrogenase from
32 *Candida Boidinii* by Site-Directed Mutagenesis of Cysteine
33 Residues. *Eur. J. Biochem.* **2000**, *267* (5), 1280–1289.
34 <https://doi.org/10.1046/j.1432-1327.2000.01123.x>.

35 (28) Okamoto, Y.; Köhler, V.; Paul, C. E.; Hollmann, F.; Ward,
36 T. R. Efficient in Situ Regeneration of NADH Mimics by an
37 Artificial Metalloenzyme. *ACS Catal.* **2016**, *6* (6), 3553–3557.
38 <https://doi.org/10.1021/acscatal.6b00258>.

Table of Contents (TOC)

TOF = 3731 h^{-1} at 313 K
